

LCLS BUNCH COMPRESSOR CONFIGURATION STUDY FOR SOFT X-RAY OPERATION

S. Li*, Y. Ding, Z. Huang, T. Maxwell, D. Ratner,
SLAC National Accelerator Laboratory, Menlo Park, USA

Abstract

The Linac Coherent Light Source (LCLS) is originally designed and commissioned with two bunch compressors (BC1 and BC2) to achieve the desired bunch length and peak current prior to the undulator line. The dispersive properties of bunch compressors enhance the growth of electron beam micro-bunching, so BC1 and BC2 provide important tuning parameters to suppress micro-bunching instability (MBI). Given the less stringent peak current requirement for soft x-ray operation, we explore new bunch compressor configurations to reduce undesired micro-bunching. New configurations include using BC1 or BC2 only, and different compression distributions between the two bunch compressors. We have developed a simplified theoretical model to characterize the micro-bunching gain under various bunch compressor configurations. Meanwhile, we require reasonable longitudinal phase space and beam current to ensure the applicability of the new schemes. We have experimentally tested the feasibility of the new configurations and obtained promising preliminary data that indicate better MBI suppression for soft x-ray operation.

INTRODUCTION

In an X-ray free electron laser (XFEL), an initial small amount of density modulation on the electron beam induces energy modulation. When the electrons go through a dispersive section, such as a bunch compressor (BC), this energy modulation converts to density modulation that is significantly larger than the initial density modulation, which is called micro-bunching instability (MBI). MBI is undesired because the wavelength (micron scale) is orders of magnitude longer than the intended X-ray radiation wavelength (nanometer or angstrom scale), and MBI results in increased slice energy spread. The laser heater at LCLS was installed to increase the initial uncorrelated energy spread in the electron beam in order to suppress MBI and lower electron beam final energy spread [1, 2]. The most effective Landau Damping of MBI occurs when the laser heater induces a Gaussian energy spread in the electrons, but the shape of the energy spread is subject to the the transverse shape of the heater laser and its transverse size relative to the electron beam size. Previous experiments have shown that for soft x-ray operation, MBI suppression becomes less effective as peak current increases [3]. Another consequence of MBI is the spectrum pedestals seen experimentally in soft x-ray self-seeding [4, 5], where the long-wavelength micro-bunching structure in the electron beam broadens the self-seeding spectrum bandwidth. Therefore, there is strong motivation

to improve MBI suppression. As described above, MBI is enhanced through dispersive sections, which implies possible new bunch compressor configurations that can further suppress MBI in addition to the laser heater. In this paper, we present a simplified theoretical model to characterize the micro-bunching gain, based on which we select useful BC configurations by tuning BC1 and BC2 parameters. Together with *LiTrack* simulations we describe a few feasible BC configurations that we have progressed through various experiments. Finally we demonstrate preliminary experimental results that show promising potential of one of the new configurations.

MBI GAIN CALCULATION

One way to characterize micro-bunching is to calculate the bunching factor growth through out the linac. The bunching factor is defined as the Fourier transform of current fluctuations. The MBI gain is defined as the bunching factor growth, $G = \left| \frac{b_f(k_f)}{b_0(k_0)} \right|$. We can express the gain through a single MBI stage as [1]

$$G(k) \approx \frac{I_0 C k_0}{\gamma I_A} \left| R_{56} \int_0^L ds \frac{4\pi Z(k_0, s)}{Z_0} \right| \times e^{-(C k_0 R_{56} \sigma_\delta)^2 / 2}, \quad (1)$$

where I_0 is the initial peak current, k_0 is the initial bunching wavenumber, R_{56} is the chicane longitudinal dispersion, L is the accelerator length, $Z_0 = 377 \Omega$ is the free space impedance, and $I_A = 17 \text{ kA}$ is the Alfvén current. In the limit $\frac{k r_b}{\gamma} \ll 1$, we have

$$Z(k) \approx \frac{i Z_0 k}{4\pi \gamma^2} \left(1 + 2 \ln \frac{\gamma}{r_b k} \right), \quad (2)$$

where r_b is the radius of the electron beam transverse cross section of a uniform beam, which we take to be $300 \mu\text{m}$ for following calculations. The total MBI gain should be integrated throughout LCLS linac machine, including all dispersion stages and accelerators. Note that even though the complete form of the gain curve is lengthy, it carries the same exponential decay factor as in Eq. 1. The details of the derivation will be presented elsewhere. This gain curve specifically depends on the following parameters: initial bunching wavenumber, compression factors, R_{56} , and beam energies at BC1 and BC2 respectively.

NEW BC CONFIGURATIONS

The nominal schematic for soft x-ray operation of LCLS is displayed in Fig. 1. Normally BC1 compresses the beam by a factor of 8, and BC2 by a factor of 4, to achieve final peak current on the order of 1 kA - 2 kA.

* siqili@slac.stanford.edu

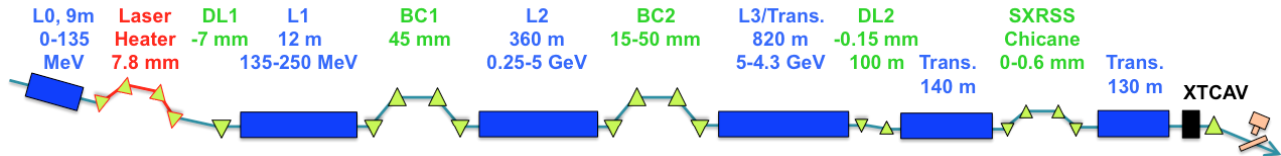


Figure 1: Diagram of LCLS schematic. For dispersive regions, the R_{56} is given in mm. Figure taken from [3].

Dispersive sections are the major contributor to MBI, therefore the most intuitive solution to suppressing MBI is to use fewer dispersive sections [6]. Beam energy is lower at BC1 than at BC2, giving a higher relative energy spread at BC1 that damps the bunching factor exponentially (Eq. 1). In this scheme, we switch off BC2 and only use BC1 to reach full compression to 1 kA final peak current, and leave L2 and L3 to do most acceleration to achieve 4 GeV final beam energy. Due to the long length of linac acceleration, this scheme has a severe practical problem where we have to use close to -90° L3 phase to cancel the energy chirp induced throughout the linac structure wakefield in order to reach a flat final phase space. The high chirp on L3 is subject to phase jitter in the machine, and therefore significantly increases energy jitter of the electron beam.

The other option is to use BC2 only. However, BC2 energy has to be lowered significantly in order to increase relative energy spread which goes into the exponential term in Eq. 1. This also creates operational challenge since the BC2 chicane is originally designed for much higher energy particles and sending beam through the chicane at a much lower energy becomes difficult operationally.

As it turns out from the gain calculation, it is still possible to use BC2 to complete most of the compression while leaving BC1 R_{56} as in the nominal setup. In this configuration, we need a smaller chirp before BC1 and a lower energy at BC2 to 700MeV to achieve sufficient MBI suppression. *LiTrack* [7] simulation further ensures the feasibility of this scheme, showing a relatively flat phase space prior to undulator entrance. One disadvantage of this scheme is the apparent double-horn structure in the current profile (lower left plot in Fig. 2). Eventually we arrive at a satisfactory solution where we lower BC1 R_{56} to reduce the double-horn structure in the current profile (lower right plot in Fig. 2) while keeping other parameters the same. All relevant parameters are tabulated in Table 1. Note that final peak current can be adjusted experimentally by varying L2 phase. L3 phase is placed at 0° to reduce energy jitter. The gain curve for the four configurations described above as compared to the regular soft x-ray set up is shown in Fig. 3.

EXPERIMENTAL RESULTS

We have obtained preliminary experimental data that show promising potential for feasibility and MBI suppression. The phase spaces are shown in Fig. 4. The “new” configuration refers to the setup with parameters in Table 1. The advantage of the new configuration is most apparently shown in the lower laser heater energy cases. From the phase space, one

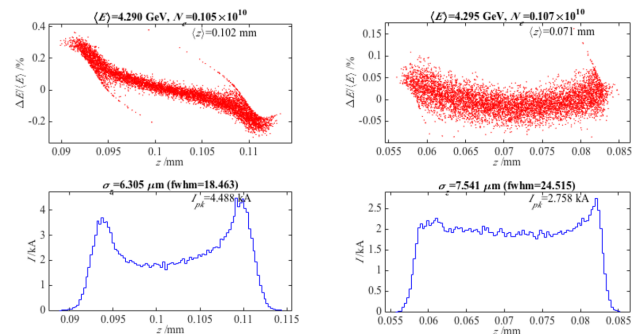


Figure 2: *LiTrack* simulation for longitudinal phase space and current profile prior to undulator entrance. The left column is BC1=45.5 mm, and the right column is BC1=35 mm. Other parameters are listed in Table 1.

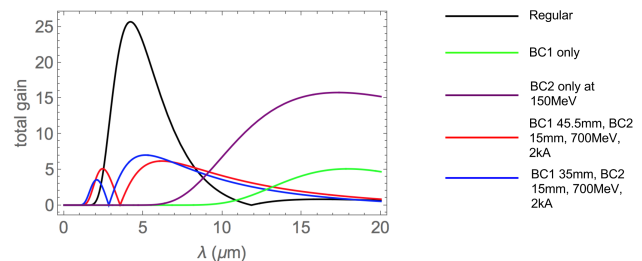


Figure 3: Gain curves as a function of final bunching wavelength for the four different configurations described in the text.

can see the micro-bunching in the new configurations shifts to longer wavelength modulation compared to the nominal setup. The detailed MBI bunching factor analysis follows the procedure described in [3], and the bunching factor is plotted in Fig. 5. The fact that the bunching factor amplitude decreases as the final peak current increases for the new configuration is also supported by the theoretical gain calculation.

Slice energy spread (SES) is another important parameter for evaluating the quality of the beam. The analysis is still work in progress and will be presented elsewhere.

CONCLUSIONS

In this paper, we have discussed the motivation of new bunch compressor configurations in order to improve micro-bunching instability suppression in addition to the use of laser heater. The gain calculation gives a theoretical start point to search for new configurations, and *LiTrack* simula-

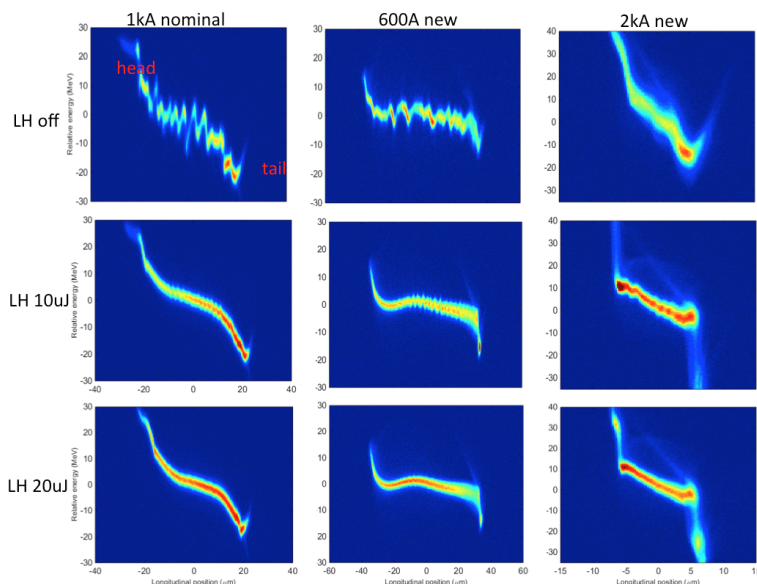


Figure 4: Example phase space from experiments. The left column is the nominal soft x-ray setup. The middle and the right column show phase space of new configurations at two different final peak currents. From top to bottom, laser heater energy increases. Bunch head is on the left in all plots.

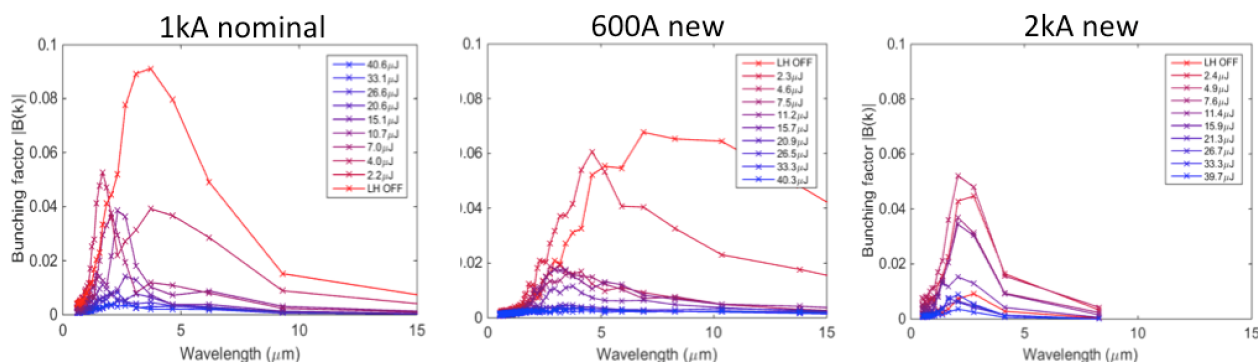


Figure 5: Bunching factor as a function of final bunching wavenumber.

Table 1: New BC Configuration Parameters

variable	value
L1X amplitude	18 MV
L1X phase	-170°
L1S phase	-15°
BC1 energy	220 MeV
BC1 current	90 A
BC1 R_{56}	35 mm
L2 phase	-60° (to achieve 2 kA)
BC2 energy	700 MeV
BC2 R_{56}	35 mm

tion serves as a guideline to ensure reasonable longitudinal phase space. We have also presented preliminary experimental results that show improved micro-bunching instability suppression, and we have demonstrated the feasibility of running LCLS with the brand new bunch compressor configuration. The prospect is to develop a more sophisticated

theoretical model to characterize the micro-bunching gain and explore potential other configurations [8]. Eventually we plan to apply the new configuration to experiments such as soft x-ray self-seeding to study its effect in suppressing the spectrum pedestal.

REFERENCES

- [1] Huang, Z. *et al.*, “Suppression of microbunching instability in the linac coherent light source”, in *Phys. Rev. ST Accel. Beams*, vol. 7.7, p. 074401, 2004.
- [2] Huang, Z. *et al.*, “Measurements of the linac coherent light source laser heater and its impact on the x-ray free-electron laser performance”, in *Phys. Rev. ST Accel. Beams*, vol. 13.2, p. 020703, 2010.
- [3] Ratner, Daniel *et al.*, “Time-resolved imaging of the microbunching instability and energy spread at the Linac Coherent Light Source”, in *Phys. Rev. ST Accel. Beams*, vol. 18.3, p. 030704, 2015.

- [4] Ratner, Daniel *et al.*, “Experimental demonstration of a soft x-ray self-seeded free-electron laser”, in *Phys. Rev. Lett.*, vol. 114.5, p. 054801, 2015.
- [5] Zhang, Zhen *et al.*, “Microbunching-instability-induced sidebands in a seeded free-electron laser”, in *Proc. of FEL'15*, Daejeon, Korea, 2016, paper WEP084, p. 741.
- [6] Di Mitri, S. *et al.*, “Suppression of microbunching instability with magnetic bunch length compression in a linac-based free electron laser”, in *Phys. Rev. ST Accel. Beams*, vol. 13.1, p. 010702, 2010.
- [7] Bane, K.L.F. and P. Emma, “LiTrack: A fast longitudinal phase space tracking code with graphical user interface.”, in *Proc. of PAC'05*, Knoxville, Tennessee, USA, paper FPAT091, p. 4266.
- [8] Di Mitri, S. and S. Spampinati, “Microbunching instability suppression via electron-magnetic-phase mixing”, in *Phys. Rev. Lett.*, vol. 112.13, p. 134802, 2014.